




## Comparing the effects of jouravskite and ettringite on the hydration of the clinker

 H.Y. Ghorab,  M.K. Mohamed ,  S.K. Mohamed

Faculty of Science, Chemistry Department, Helwan University, (Cairo, Egypt)  
: mohamed.kamal@science.helwan.edu.eg

---

Received 06 August 2022  
Accepted 09 December 2022  
Available on line 06 March 2023

**ABSTRACT:** Manganese enters the clinker from alternative fuel and alternative raw materials. It is present in the iron ores utilized in the cement burning and is found in the slags employed as supplementary cement materials. The jouravskite, as a member of the ettringite family, may form in limestone cement when exposed to sulfate media. To understand its effect on the hydration process, the expansion of small cylindrical clinker pastes doped with synthesized jouravskite and ettringite in magnesium sulfate solutions was measured with a micrometer; and the compressive strength of representative cubes was monitored. The phases formed were characterized by means of X-ray diffraction, infrared spectroscopy and scanning electron microscopy. The jouravskite is found to be a strong retarder for clinker hydration probably due to its adsorption on the cement hydrates.

**KEY WORDS:** Jouravskite; Ettringite; Clinker; Hydration; Sulfate solution.

**Citation/Citar como:** Ghorab, H.Y.; Mohamed, M.K.; Mohamed, S.K. (2023) Comparing the effects of jouravskite and ettringite on the hydration of the clinker. *Mater. Construcc.* 73 [349], e303. <https://doi.org/10.3989/mc.2023.300222>.

**RESUMEN:** *Comparando los efectos de la jouravskita y la etringita en la hidratación del clinker.* El manganeso ingresa al clinker a partir de combustibles alternativos y materias primas alternativas. Está presente en los minerales de hierro utilizados en la combustión del cemento y se encuentra en las escorias empleadas como materiales complementarios del cemento. La jouravskita, como miembro de la familia de la etringita, puede formarse en cementos de piedra caliza cuando se expone a medios ricos en sulfatos. Para comprender su efecto en el proceso de hidratación, se midió con un micrómetro la expansión de pequeñas pastas cilíndricas de clinker dopadas con jouravskita y etringita sintetizadas en soluciones de sulfato de magnesio, y se monitoreó la resistencia a la compresión de cubos representativos. Las fases formadas se caracterizaron mediante difracción de rayos X, espectroscopia infrarroja y microscopía electrónica de barrido. Se encuentra que la jouravskita es un fuerte retardador de la hidratación del clinker, probablemente debido a su adsorción en los hidratos de cemento.

**PALABRAS CLAVE:** Jouravskita; Etringita; Clíinker; Hidratación; Solución de sulfato.

**Copyright:** ©2023 CSIC. This is an open-access article distributed under the terms of the Creative Commons Attribution 4.0 International (CC BY 4.0) License.

## 1. INTRODUCTION

According to World Bank data (1), the world generates 2 billion tons of municipal solid waste annually and is expected to increase to 3.4 billion metric tons by 2050. This problem was partially solved by the employment of the wastes in the cement industry because of the high temperature of the kiln and the suitable chemistry of the clinker. This strategy was implemented in the early 1990s (2). Municipal, industrial, and agricultural wastes are now largely used in the cement plants. For the cement manufacturers, the advantages of their use are cost savings, conservation of natural resources, and minimization of greenhouse gas emissions. These applications have, however, influenced the cement manufacturing process and the properties of the product (3-5). The clinker absorbs the ashes and entraps the non-volatile and semi-volatile heavy metals in the crystal lattice of its phases. Several trace elements available in the ashes, which were not present in conventional raw materials and regular fuels, are incorporated in the clinker; manganese is the focus of this paper. The World Bank data (1) shows that the world generates ~2 billion tons of municipal solid waste annually and is expected to increase to 3.4 billion metric tons by 2050. This problem was partially solved by the employment of the wastes in the cement industry because of the high temperature of the kiln and the suitable chemistry of the clinker. This strategy was implemented in the early 1990s (2). Municipal, industrial, and agricultural wastes are now largely used in the cement plants. For the cement manufacturers, the advantages of their use are cost savings, conservation of natural resources, and minimization of greenhouse gas emissions. These applications have, however, influenced the cement manufacturing process and the properties of the product (3-5). The clinker absorbs the ashes and entraps the non-volatile and semi-volatile heavy metals in the crystal lattice of its phases. Several trace elements that are found in the ashes but not in regular raw materials and fuels are added to the clinker. This paper will focus on manganese. Furthermore, the amount of manganese oxides in cement made from primary raw materials was rarely greater than 0.2% (6). Their concentrations in the cements produced with alternative fuels and raw materials might attain ~0.9% (3). Manganese is present in a significant amount in the iron ores used to reduce the clinkering temperature (7). Its content in the blast furnace slag cement may reach 5%. Studies are reported in the literature (8–11) on the use of silicon-manganese slag with ~ 10% MnO, as well as steel slag, which has manganese in its structure, as cement replacement materials. The effect of manganese on the clinker hydration process must thus be investigated. Manganese appears in several ox-

idation states ( $M^{2+}$ ,  $Mn^{3+}$ , and  $Mn^{4+}$ ) in Portland cement clinker (12–15). Its presence in the clinker can be summarized as follows: The replacement of  $Ca^{2+}$  by  $Mn^{2+}$  is possible due to the similarity of their ionic radii (0.91 and 0.99).  $Mn^{3+}$  replaces  $Fe^{3+}$  preferentially in  $C_4AF$  and forms  $Ca_2AlMnO_5$ . Its substitution for  $Al^{3+}$  in the  $C_3A$  is limited, and the  $C_3A$  content is reduced in parallel with its incorporation in the ferrite phase (16). In the  $C_3S$  and  $C_2S$  phases,  $Si^{4+}$  is difficultly replaced by  $Mn^{4+}$ , with the  $C_2S$  phase having a higher capacity for doping, but in the presence of excess Mn,  $2CaO.MnO_2$  forms.

On the other hand, the strength of cement decreases when the concentration of  $Mn_2O_3$  is higher than 0.5% (1, 17). Manganese was found to activate the hydration of the ferrite phase but reduce the strength of the calcium silicate hydrates (3).

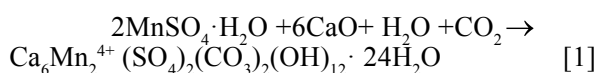
Few publications are found on the type of manganese salts formed during cement hydration. The tetravalent oxidation state of manganese is the most stable state in neutral and alkaline solutions (18). The jouravskite,  $Ca_3Mn^{4+}(SO_4)(CO_3)(OH)_6.12H_2O$ , is an interesting salt in cement chemistry because it is an ettringite with isostructural similarities to thaumasite (19). Its structure is characterized by the presence of columns composed of  $[Ca_3Mn^{4+}(OH)_6(H_2O)_{12}]^{4+}$  formed by alternating  $Mn(OH)_6$  octahedra and triplets of Ca-centered eightfold polyhedra  $Ca(OH)_4(H_2O)$ . The  $SO_4$  tetrahedra and  $CO_3$  triangles are located among the columns, and all O atoms of these groups are involved in a system of hydrogen bonds (20). It is expected that jouravskite will form in limestone-bearing cements with enough manganese content exposed to sulphate media. To understand its nature, the expansion of a clinker doped with a synthesized jouravskite salt in sulphate solution was compared with that of a clinker doped with ettringite (21). Previous research (22, 23) demonstrated a significant length change in sodium sulphate solutions of a synthesized ettringite as well as clinker doped with ettringite. The clinker sample deteriorated after 60 days of exposure to a 1 molar solution. In the present work, measurements are carried out using the self-designed methods applied in the previous research as follows (22, 23): The length change of the clinker pastes was recorded for small cylindrical samples using an accurate micrometer, and the compressive strength of the hardened pastes was measured on 1x1x1 inch cubes.

## 2. EXPERIMENTAL PROCEDURE

### 2.1 Preparation

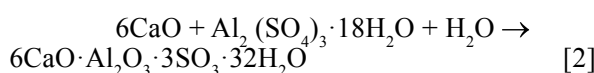
The jouravskite salt was prepared from chemically pure manganous sulfate solution and lime

dissolved in sugar solution to increase its solubility (Equation [1]) (24).



The lime/sugar solution was added dropwise to the sulfate solution with continuous stirring. The beaker was covered with a black plastic sheet, stirred overnight, then vacuum filtered and left in a desiccator for two days.

The ettringite was prepared from aluminum sulfate solution and lime at room temperature (Equation [2]) (23).



The lime suspension was added to the sulfate solution, stirred for 24 hours, and then filtered off. The precipitate was removed by vacuum filtration, rinsed with distilled water followed by isopropyl alcohol, and then dried at 50°C for 1 day.

Wet chemical analysis (21) and a Philips X-ray spectrometer model PW/1710 were used to determine the chemical composition of jouravskite. An X-ray diffraction apparatus (X'PERT MPD) and a Philips diffractometer with a nickel filter and copper K- radiation were used to identify the structures of jouravskite and ettringite. The functional groups were analyzed with the Fourier transform infrared spectrometer, FTIR-4100 Type A. The morphology of selected samples was examined using a scanning electron microscope, FEI Type QUANTA 250, equipped with a Field Emission Gun (FEG) with a 30 kV accelerating voltage.

## 2.2 Effect on the clinker

The effect of jouravskite and ettringite on the hydration of the clinker was studied by measuring the expansion of clinker pastes doped with each salt keeping the  $\text{SO}_3$  concentration equal to 5%. This concentration was found to have no negative influence on the cement at room temperature (23). The total manganese concentration in the jouravskite-doped clinker was 1.49  $\text{Mn}_2\text{O}_3\%$ . The expansion of the pastes was measured using a self-designed method employed in previous work (22, 23). The pastes were cast in cylindrical plastic molds with a 20-mm diameter and 40 mm height, using a water/solid ratio of 0.3. The samples were covered with a plastic sheet for one day, then demolded. The zero-reading was recorded by measuring the length of the hardened cylinder using a micrometer with an accuracy of 0.01 mm. The cylindrical samples were cured in 0.01, 0.1, and 1% magnesium sulfate solutions at room temperature, and their length change was re-

corded at 60 days. The phases formed in the bulk of the samples were studied using X-ray diffraction, infrared spectroscopy, and a scanning electron microscope. The compressive strength of the pastes was measured for 1x1x1 inch cubic samples cast in steel molds and cured as before. Readings were recorded after 28 and 60 days.

## 3. RESULTS

### 3.1 Characterization

The X-ray diffraction patterns of the synthesized jouravskite are depicted in Figure 1. They show d-value lines at 9.52, 5.52, 4.91, 3.88, 3.59, 3.44, 3.09, 2.76, 2.60, 2.21, 1.92, 1.79, 1.68, and 1.60 Å, which corresponds to jouravskite database (25, 26).

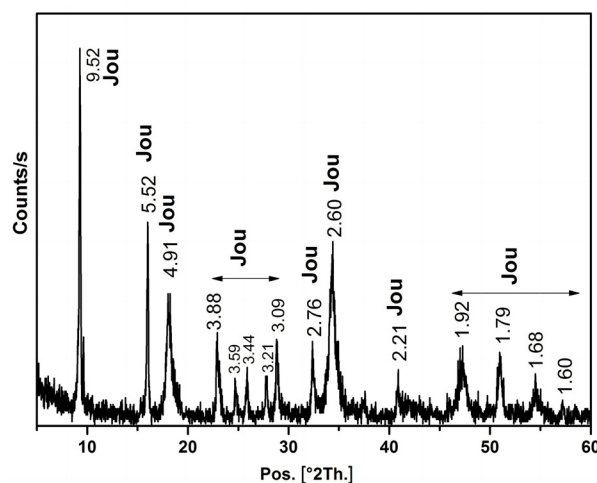


FIGURE 1. The X-ray diffraction patterns of jouravskite (Jou).

Wet chemically (21) and using X-ray fluorescence, the oxide composition of the synthesized jouravskite, with the theoretical formula  $\text{Ca}_3\text{Mn}^{4+}(\text{SO}_4)(\text{CO}_3)(\text{OH})_6 \cdot 12(\text{H}_2\text{O})$ , was determined. The results obtained are very close to each other and accord with the theoretical value (Table 1).

TABLE 1. Chemical composition of jouravskite (wt. %).

Oxide	Theoretical	Wet Chemically	XRF
CaO	25.20	25	25.22
MnO <sub>2</sub>	13.02	12.5	13.04
SO <sub>3</sub>	17.99	17.4	17.94
CO <sub>2</sub>	3.30	3.6	3.37
H <sub>2</sub> O	40.49	41.5	40.43

The infrared spectra of Figure 2 indicate a strong band of OH/portlandite at 3642  $\text{cm}^{-1}$ . The stretching

and bending modes of OH/water are found at 3390 and 1645  $\text{cm}^{-1}$  and the CO bands of carbonate are at 1473 and 1411  $\text{cm}^{-1}$ . The strong band observed at 1099  $\text{cm}^{-1}$  is attributed to the stretching vibration mode of S-O, and that at 620  $\text{cm}^{-1}$  is due to the bending vibration. The bands identified at 573 and 550  $\text{cm}^{-1}$  belong to  $\text{Mn}^{4+}$ -O stretching vibrations. These data agree with the literature (20).

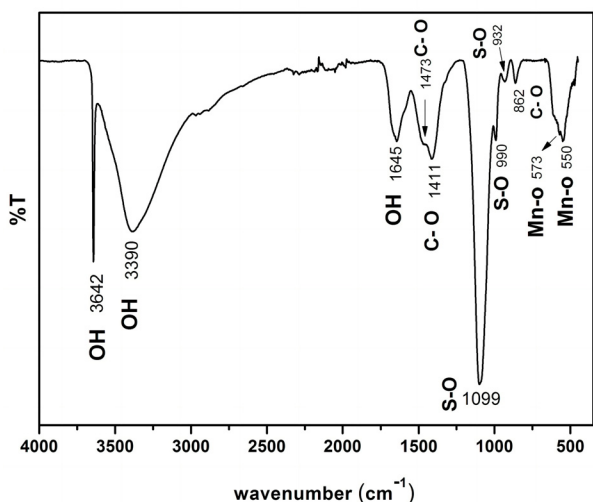


FIGURE 2. The Infrared spectra of jouravskite.

The morphology of the salt shows rounded columnar shaped particles of different sizes lying in the range of 3-4 microns (Figure 3).

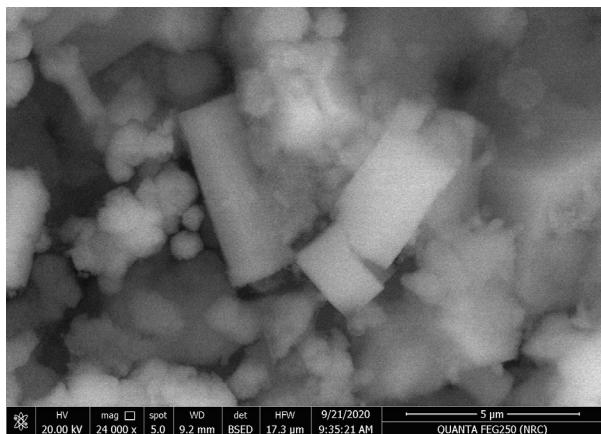


FIGURE 3. The scanning electron micrograph of the prepared jouravskite salt.

All of the characteristics of the prepared ettringite salt were consistent with the literature.

TABLE 2. The chemical composition of the clinker (wt.%).

	$\text{SiO}_2$	$\text{Al}_2\text{O}_3$	$\text{Fe}_2\text{O}_3$	CaO	MgO	$\text{Na}_2\text{O}$	$\text{K}_2\text{O}$	$\text{SO}_3$	F. L.	Cl	LOI
CEM I 42.5 R	20.83	5.07	3.91	65.05	3.19	0.32	0.17	0.74	1.32	0.01	3.7

Tables 2 and 3 illustrate the chemical composition of the clinker. Its X-ray diffraction patterns, and its infrared spectra are shown in Figures 4 and 5. All the characteristic d-value lines of the clinker phases are represented in the diffractogram. As expected, no hump is observed in the background of the figure; the hump reflects the hydration of the sample and the presence of amorphous products.

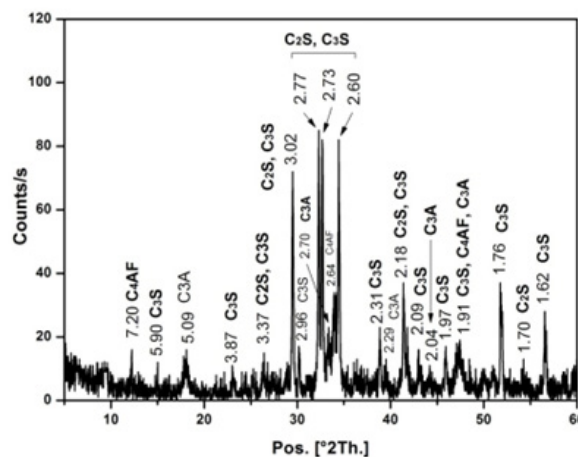


FIGURE 4. The X-ray diffraction patterns of the clinker.

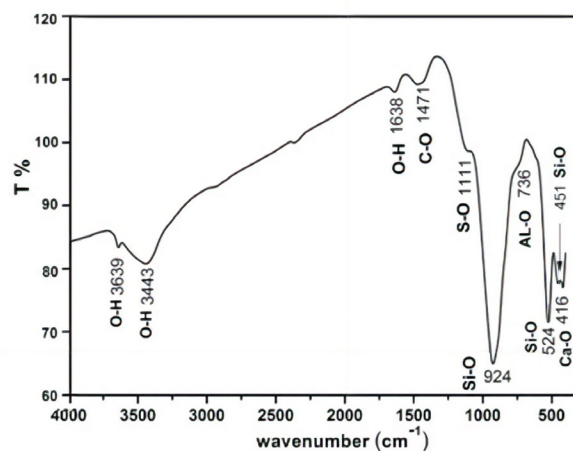


FIGURE 5. The infrared spectra of the clinker.

The infrared spectrum of the clinker indicates that a slight hydration and carbonation of the clinker occurred in the sample; the respective bands appear in the range of 3500 and 1470  $\text{cm}^{-1}$  respectively. Weak shoulders of S-O and Al-O are detected at 1111 and 736  $\text{cm}^{-1}$ , and the Si-O frequencies are observed at 924 and 451  $\text{cm}^{-1}$ .

TABLE 3. The phases composition of the clinker (wt.%).

C <sub>3</sub> S	C <sub>2</sub> S	C <sub>3</sub> A	C <sub>4</sub> AF
66.80	9.41	6.82	11.89

### 3.2 Effect on the clinker

Figure 6a shows the expansion behavior of the clinker pastes doped with jouravskite in 0.01, 0.1, and 1% magnesium sulfate solutions at room temperature. The expansion of the clinker doped with ettringite is illustrated in Figure 6b. The results show that no significant change occurs in the length of the clinker/jouravskite curve over the 60-day exposure time; the clinker/ettringite pastes, however, undergo noticeable expansion in 0.1 and 1% magnesium sulfate solutions.

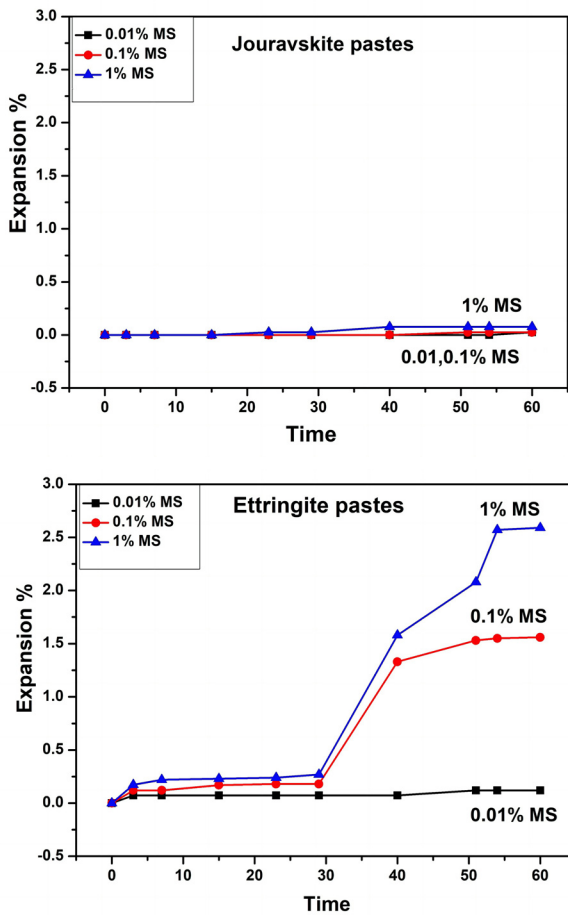


FIGURE 6. Expansion of the clinker pastes doped with a) jouravskite- b) ettringite in 0.01, 0.1, 1 % magnesium sulfate at room temperature.

Figure 7 illustrates the X-ray diffractogram of a sample taken from the bulk of the clinker/ ettringite paste cured in a 1% magnesium sulfate solution for 60 days. The diffractogram of the clinker/

jouravskite paste treated under similar conditions is shown in Figure 8. The results indicate the presence of the ettringite d-values at 9.63, 5.56A and others, beside gypsum and portlandite. In this figure, the clinker patterns are weak, which means that progressive hydration took place in the sample. This is supported by the presence of a hump in the two-theta range of 25 to 35 degrees, which reflects the presence of amorphous products in the sample. Figure 8 shows the presence of jouravskite patterns at 9.55 and 5.55 Å, beside a moderate peak at 4.95 Å attributed to portlandite and jouravskite. Well-defined lines of the anhydrous clinker phases appear at 3.02, 2.76, 2.73, and 2.59 Å. The absence of a hump in the two-theta range of 25 to 35 degrees means that the hydration process of the clinker is retarded.

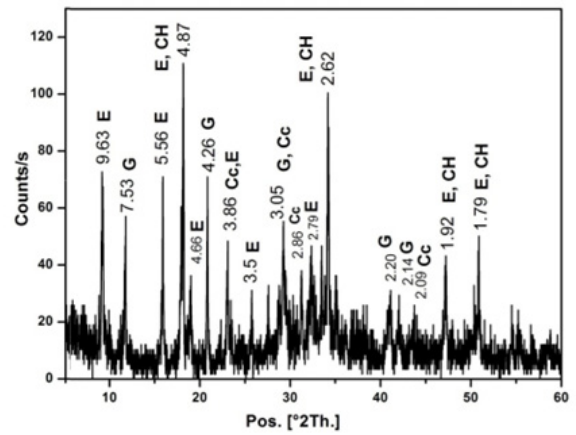


FIGURE 7. The X-ray diffraction patterns of the bulk of clinker/ ettringite paste cured in 1% magnesium sulfate solution for 2 months. (E=Ettringite, CH= Portlandite, G=Gypsum, Cc=Calcite).

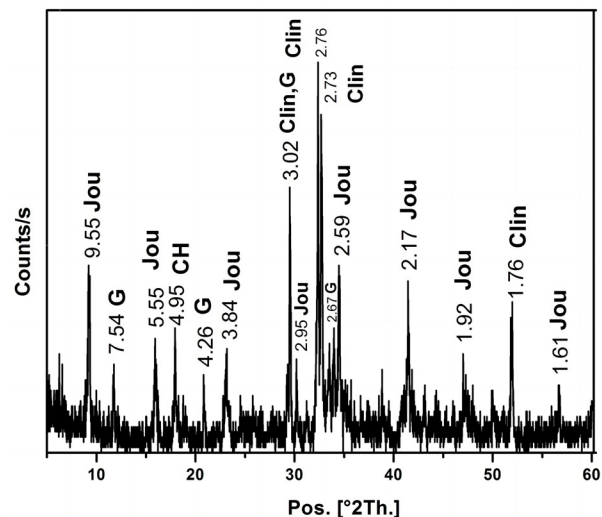


FIGURE 8. The X-ray diffraction patterns of the bulk of clinker/ jouravskite paste cured in 1% magnesium sulfate solution for 2 months (Jou= Jouravskite, G=Gypsum, Clin= Clinker, CH=Portlandite).

The scanning electron micrograph of the paste cured for 60 days at room temperature in 1% magnesium sulphate solution shows a coated layer formed on the surface of the clinker phases (Figure 9). This sample's infrared spectra show a weak stretching vibration of the OH<sup>-</sup> group of calcium hydroxide at 3640 cm<sup>-1</sup> (Figure 10); the bands detected at 989 and 940 cm<sup>-1</sup> are assigned to the stretching vibration of Si-O; and the band detected at 539 cm<sup>-1</sup> is assigned to Mn-O.

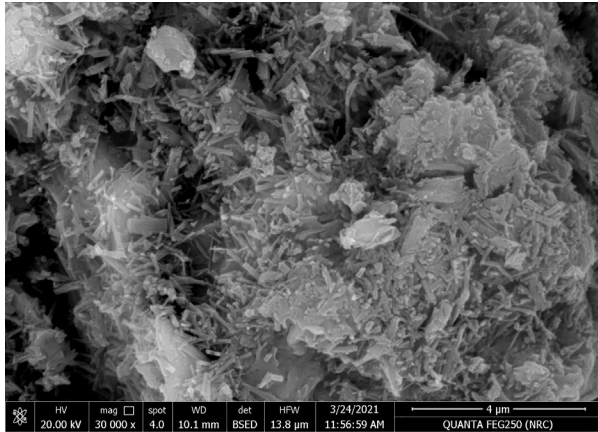


FIGURE 9. The scanning electron micrograph clinker/jouravskite pastes cured 60 days in 1% magnesium sulfate at room temperature indicating a layer probably coating the clinker phases.

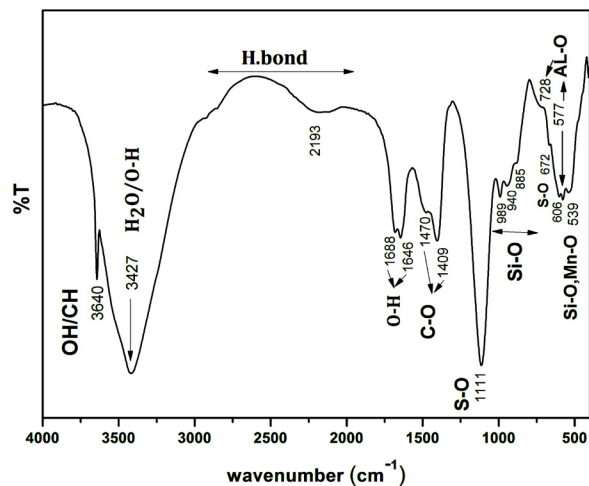


FIGURE 10. Infrared spectra of the bulk of clinker/ jouravskite paste cured 60 days in 1% magnesium sulfate solution at room temperature.

The 28 and 60-days compressive strength curves of the clinker/jouravskite and the clinker/ettringite pastes in 0.01, 0.1, 1 % magnesium sulfate at room temperature were identical. Typical curves are depicted in Figure 11 next to those of the reference pastes for comparison. The results show very low compressive strength values for the clinker/

jouravskite pastes, which reach zero at 60 days. The values of the clinker/ ettringite are low as well but are slightly higher than those of the jouravskite. The reference sample shows a value of 18 N/mm<sup>2</sup> after one month and increases to 25 N/mm<sup>2</sup> after 60 days.

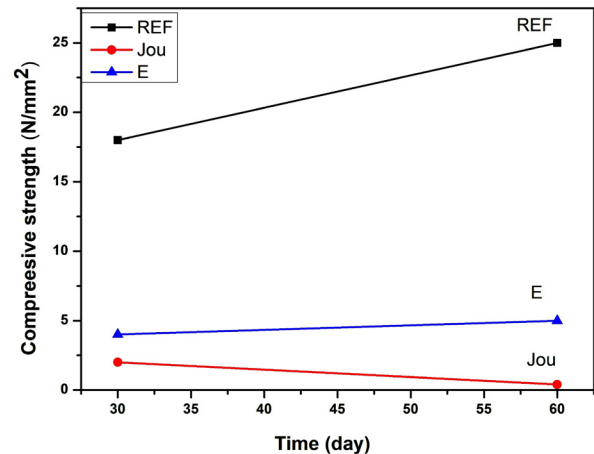


FIGURE 11. Typical curves for the compressive strength of the clinker/jouravskite (jou)-, the clinker/ ettringite (E) and the reference pastes in 0.01, 0.1, 1 % magnesium sulfate at room temperature.

#### 4. DISCUSSION

The ettringite ( $\text{Ca}_6[\text{Al}(\text{OH})_6]_2(\text{SO}_4)_3 \cdot 24\text{H}_2\text{O}$ ), and thaumasite ( $\text{Ca}_6[\text{Si}(\text{OH})_6]_2(\text{SO}_4)_2(\text{CO}_3)_2 \cdot 24\text{H}_2\text{O}$ ) salts are known to damage cement and concrete in sulfate media. The structure of ettringite is composed of columns of central trivalent aluminum ions surrounded octahedrally by hydroxyl ions attached to the 8-coordinated calcium ions. The expansive properties take place in the presence of excess sulfate, lime, and humidity at room temperature. The sulfates enter the channels between the columns and cause expansion. The source of sulfate may be internal or external (27, 28).

In thaumasite, tetravalent silicon is present as a central ion in the octahedra instead of aluminum. It is responsible for the deterioration of cement systems in carbonate and sulfate media at low temperatures (<15°C). The mechanism of its formation is explained as follows: In the presence of carbonate, the pH-value of the system is reduced, the calcium silicate hydrates, and ettringite decomposes. Thaumasite forms with the resupply of lime and the rise of the value. To allow the formation of the octahedral arrangement of OH<sup>-</sup> ions around the highly polarizing Si, the existence of a transition intermediate state was proposed (29). This mechanism is favored by low temperatures because of the increased solubility of lime. The intermediate phase was identified (30) as a carbonated silicate phase incorporating relics of ettringite. It shows an IR shoulder at 1030 cm<sup>-1</sup>

instead of the pure Si-O band usually appearing at  $980\text{ cm}^{-1}$ . This band disappears with the supply of lime, and the formation of thaumasite. The formation of thaumasite is not accompanied by an expansion behavior like ettringite (31), but the surface of hardened cement systems exposed to sulphate separates and further layers deteriorate.

The effect of jouravskite ( $\text{Ca}_6[\text{Mn}(\text{OH})_6]_2(\text{SO}_4)_2(\text{CO}_3)_2 \cdot 24\text{H}_2\text{O}$ ) on cement is rarely discussed in the literature, and its formation mechanism is not explained. The present work shows that it is a strong retarder for the hydration of the clinker.

The major product of the hydration of the silicate phases in cement is the calcium silicate hydrate gel. This gel is a mixture of poorly crystallized particles with a structure far from equilibrium. It is thermodynamically unstable at ambient temperature. When pH approaches 12.5, portlandite precipitates from solutions. Calcium hydroxide influences the morphological and structural features of C-S-H (32), and a tightly bound bi-layer of calcium ions forms with the negatively charged C-S-H surface (33, 34).

Heavy metals will be adsorbed on the hydration products if the amount is sufficient precipitation may occur on the surfaces of the CSH phases because of the unsatisfied charges. The cement grains are then coated with salts of the heavy metals. The saturation indices of the low-solubility species of these metals are very high, and the spontaneous nucleation of the salts occurs very quickly. Metals that form the least soluble hydroxides retard the hydration reactions, inhibit their nucleation and growth, and in some cases enhance the silicate polymerization (35, 36). The more soluble hydroxides exhibit only a slight degree of retardation, and metals that form soluble hydroxides behave as accelerators of cement hydration. In general, heavy metals are considered inhibitors of  $\text{C}_3\text{S}$ ; some of them retard early hydration and then act as accelerators at later ages.

The carbonation process might change the characteristics of the C-S-H phases and increases their capacity for retaining heavy metal cations and heavy metal hydroxyl ions, because of the large surface area and the meta-stability of decalcified C-S-H gel (34). The jouravskite shall precipitate if enough sulfate, carbonate, hydroxide, calcium, and manganese are available.

The jouravskite was added as an already-formed salt in the current work. Its effect on the clinker hydration is therefore explained by adsorption rather than precipitation from the individual soluble ions. The morphology of the hydration products in the clinker-jouravskite system after 60 days of immersion in 1% magnesium sulphate solution is fascinating (Figure 9) The coated layer of the cement grains is composed of particles with dimensions less than one micron. The jouravskite particles in Figure 3 are seen to be of greater size. This observation indicates that a certain interaction took place between

the jouravskite and the cement grains in the magnesium sulfate solution. The amount of portlandite in the system was very low at 60 days, as determined by infrared, indicating that clinker hydration was inhibited.

Because of the similarity between the composition of jouravskite and thaumasite, the availability of carbonate ions for their formation must be strictly considered. The jouravskite is expected to form in limestone cement and in carbonated atmosphere of ordinary Portland cement exposed to sulfate media. The low temperature required for thaumasite formation in jouravskite is unclear.

## 5. CONCLUSIONS

- The concentration of manganese in the clinker must be regularly monitored
- Jouravskite is a strong retarder for the hydration of Portland cement clinker
- The formation of jouravskite is probable in Portland limestone cements, and in carbonated ordinary Portland cement exposed to sulfate media
- The manganese can be provided from the alternative fuels and alternative raw materials used in the cement manufacture process, and the slag can be added as a mineral admixture in cements.

## ACKNOWLEDGEMENT

The authors would like to thank Helwan University for the financial support and research facilities.

## AUTHORS CONTRIBUTION

Conceptualization: H.Y. Ghorab, M.K. Mohamed. Data curation: M.K. Mohamed, H.Y. Ghorab. Formal analysis H.Y. Ghorab M.K. Mohamed. Funding acquisition: H.Y. Ghorab, M.K. Mohamed, S.K. Mohamed. Investigation: H.Y. Ghorab, M.K. Mohamed. Methodology: M.K. Mohamed, H.Y. Ghorab. Project administration: H.Y. Ghorab. Software: M.K. Mohamed. Validation: M.K. Mohamed, H.Y. Ghorab. Visualization: H.Y. Ghorab, M.K. Mohamed. Writing, original draft: H.Y. Ghorab, M.K. Mohamed, S.K. Mohamed. Writing, review & editing: H.Y. Ghorab, M.K. Mohamed, S.K. Mohamed.

## REFERENCES

1. Global Waste Statistics (2022) Waste Statistics / By Cheapa Waste.
2. Chatterjee, A.; Sui, T. (2019) Alternative fuels-Effects on clinker process and properties. *Cem. Concr. Res.* 123, 105777. <https://doi.org/10.1016/j.cemconres.2019.105777>.
3. Shimosaka, K.; Inoue, T.; Tanaka, H.; Kishimoto, Y. (2007) Influence of minor elements in clinker on the properties of cement: a new approach for application to commercial cement manufacturing. *Trans. Mater. Res. Soc. Japan.* 32 [3], 647-652. <https://doi.org/10.14723/tmrj.32.647>.
4. Achterbosch, M.; Bräutigam, K.R.; Hartlieb, N.; Kupsch, C.M.; Richers, U.; Stemmermann, P.; Gleis, M. (2003) Heavy metals in cement and concrete resulting from the

- co-incineration of wastes in cement kilns with regard to the legitimacy of waste utilisation. Karlsruhe: Forschungszentrum Karlsruhe GmbH.
5. Ludwig, H.M.; Zhang, W. (2015) Research review of cement clinker chemistry. *Cem. Concr. Res.* 78, 24-37. <https://doi.org/10.1016/j.cemconres.2015.05.018>.
  6. Lea, F.M. (1970) *The Chemistry of Cement and Concrete*. 3<sup>rd</sup> Edition, Edward Arnold Ltd. London. 76 (1970).
  7. Saidi, I.; Ben Abdelmalek, J.; Ben Said, O.; Chicharo, L.; Beyrem, H. (2020) Chemical composition and heavy metal content of portland cement in northern tunisia. *Iran. J. Chem. Chem. Eng. (IJCCE)*. 39 [3], 147-158.
  8. Nath, S.K.; Randhawa, N.S.; Kumar, S. (2022) A review on characteristics of silico-manganese slag and its utilization into construction materials. *Resour. Conserv. Recycl.* 176, 105946. <https://doi.org/10.1016/j.resconrec.2021.105946>.
  9. Saly, F.; Guo, L.; Ma, R.; Gu, C.; Sun, W. (2018) Properties of steel slag and stainless steel slag as cement replacement materials: a comparative study. *J. Wuhan Univ. Technol. Mater. Sci. Ed.* 33 [6], 1444-1451. <https://doi.org/10.1007/s11595-018-1989-3>.
  10. Anjali, P.; Sajitha Beegom, A. (2022) A study on the utilization of activated steel slag as partial replacement of cement in concrete. *Int. J. Eng. Res. Technol. (IJERT)*. 11 [01].
  11. Wulfert, H.; Keyssner, M.; Ludwig, H.M.; Adamczyk, B. (2013) Metal recovery and conversion of steel slag into highly reactive cement components. *ZKG. Int. Deutsche Ausgabe*. 9, 34-40 (1995).
  12. Puertas, F.; Glasser, F.P.; Blanco-Varela, M.T.; Vaquez, T. (1988) Influence of the kiln atmosphere on manganese solid solution in Ca<sub>3</sub>SiO<sub>5</sub> and Ca<sub>2</sub>SiO<sub>4</sub>. *Cem. Concr. Res.* 18 [5], 783-788. [https://doi.org/10.1016/0008-8846\(88\)90103-2](https://doi.org/10.1016/0008-8846(88)90103-2).
  13. Puertas, F.; Blanco, M.T.; Vázquez, T. (1989) Manganese substitutions into the portland cement clinker phases. *Mater. Construcc.* 39 [214], 19-30. <https://doi.org/10.3989/mc.1989.v39.i214.806>.
  14. Puertas, F.; Varela, M.B.; Dominguez, R. (1990) Characterization of Ca<sub>2</sub>AlMnO<sub>5</sub>. A comparative study between Ca<sub>2</sub>AlMnO<sub>5</sub> and Ca<sub>2</sub>AlFeO<sub>5</sub>. *Cem. Concr. Res.* 20 [3], 429-438. [https://doi.org/10.1016/0008-8846\(90\)90033-T](https://doi.org/10.1016/0008-8846(90)90033-T).
  15. Diouri, A.; Boukhari, A.; Aride, J.; Puertas, F.; Vázquez, T. (1997) Stable Ca<sub>3</sub>SiO<sub>5</sub> solid solution containing manganese and phosphorus. *Cem. Concr. Res.* 27 [8], 1203-1212. [https://doi.org/10.1016/S0008-8846\(97\)00110-5](https://doi.org/10.1016/S0008-8846(97)00110-5).
  16. Tao, Y.; Zhang, W.; Shang, D.; Xia, Z.; Li, N.; Ching, W.Y.; Hu, S. (2018) Comprehending the occupying preference of manganese substitution in crystalline cement clinker phases: A theoretical study. *Cem. Concr. Res.* 109, 19-29. <https://doi.org/10.1016/j.cemconres.2018.04.003>.
  17. Lea's. (1998) *Chemistry of cement and concrete*. fourth edition. ISBN 0340 565896. Reprinted by Butterworth-Heinemann.
  18. Cotton, F.A.; Wilkinson, G.; Murillo, C.A.; Bochmann, M. (1999) *Advanced inorganic chemistry*. John Wiley and Sons, Inc.
  19. Jouravskite: Mineral information, data and localities.
  20. Chukanov, N.V.; Zubkova, N.V.; Pautov, L.A.; Göttlicher, J.; Kasatkin, A.V.; Van, K.V.; Pushcharovsky, D.Y. (2019). Jouravskite: refined data on the crystal structure, chemical composition and spectroscopic properties. *Phys. Chem. Miner.* 46 [4], 417-425. <https://doi.org/10.1007/s00269-018-1012-8>.
  21. Mohamed, M.K.M. (2022) Studies on some important salts formed in Portland cement: Thaumassite and ettringite-similar phases. Ph.D. Thesis, Helwan University Cairo Egypt.
  22. Ghorab, H.Y.; Zayed, A.M.; Mohamed, A.S.; Abdel Tawab, Y.; Mabrouk, M.R.; Ahmed, H.E.H. (2007) Factors affecting the sulfate expansion in cement systems. 12<sup>th</sup> Inter. Cong. Chem. Cem. (ICCC). Montreal, Canada, TH4-12.4.
  23. Mohamed, A.S. (2006) Studies on the expansion behavior of ettringite in pure systems and in cement pastes. M.Sc. thesis Helwan University, Cairo, Egypt.
  24. Norman, R.L.; Dann, S.E.; Hogg, S.C.; Kirk, C.A. (2013) Synthesis and structural characterisation of new ettringite and thaumasite type phases: Ca<sub>6</sub> [Ga (OH) 6· 12H<sub>2</sub>O] 2 (SO<sub>4</sub>) 3· 2H<sub>2</sub>O and Ca<sub>6</sub> [M (OH) 6· 12H<sub>2</sub>O] 2 (SO<sub>4</sub>) 2 (CO<sub>3</sub>) 2, M= Mn, Sn. *Solid. State. Sci.* 25, 110-117. <https://doi.org/10.1016/j.solidstatesciences.2013.08.006>.
  25. Granger M.; Protas, J. (1969) Determination et etude de la structure cristalline de la jouravskite Ca<sub>2</sub>MnIV(SO<sub>4</sub>)(CO<sub>3</sub>)(OH)\*12(H<sub>2</sub>O). *Acta. Crystallogr.* B25 1943-1951 Locality: Tachgagalt mine, Morocco. Database code amcsd 0009362.
  26. Gaudefroy, C.; Permingeat, F. (1965) La jouravskite, une nouvelle espèce minérale. *Bull. Soc. fr. mineral. Cristallogr.* 88, 254-262. Reference code 00-018-0668.
  27. Scrivener, K.; Skalny, J.P. (2005) Conclusions of the international RILEM TC 186-ISA workshop on internal sulfate attack and delayed ettringite formation (4-6 September 2002, Villars, Switzerland). *Mater. Struct.* 38 [6], 659-663. <https://doi.org/10.1007/BF02481597>.
  28. Whittaker, M.; Black, L. (2015) Current knowledge of external sulfate attack. *Adv. Cem. Res.* 27 [9], 532-545. <https://doi.org/10.1680/adcr.14.00089>.
  29. Bensted, J. (2003). Thaumassite—direct, woodfordite and other possible formation routes. *Cem. Concr. Compos.* 25 [8], 873-877. [https://doi.org/10.1016/S0958-9465\(03\)00115-X](https://doi.org/10.1016/S0958-9465(03)00115-X).
  30. Ghorab, H.Y.; Zahran, F.S.; Kamal, M.; Meawad, A.S. (2018). On the durability of portland limestone cement: Effect of pH on the thaumasite formation. *HBRC J.* 14 [3], 340-344. <https://doi.org/10.1016/j.hbrj.2017.04.002>.
  31. Ghorab, H.Y.; Mabrouk, M.R.; Abd Elnaby, S.F.; Youstri, K.M.; Ahmed, H.H.; Herfort, D.; Osman, Y.A. (2014). The suitability of portland limestone cement for use in construction applications in Egypt. *Cem. Inter.* 12, 70-77.
  32. Dweck, J.; Ferreira da Silva, P.; Silva Aderne, R.; Büchler, P.; Cartledge, F.K. (2003) Evaluating cement hydration by non-conventional DTA; An Application to Waste Solidification. *J. Therm. Anal. Calorim.* 71 [3], 821-827. <https://doi.org/10.1023/a:1023322108940>.
  33. Chen, Q.Y.; Tyrer, M.; Hills, C.D.; Yang, X.M.; Carey, P. (2009) Immobilisation of heavy metal in cement-based solidification/stabilisation: A review. *Waste. Manag.* 29 [1], 390-403. <https://doi.org/10.1016/j.wasman.2008.01.019>.
  34. Yousuf, M.; Mollah, A.; Vempati, R.K.; Lin, T.C.; Cocke, D.L. (1995) The interfacial chemistry of solidification/stabilization of metals in cement and pozzolanic material systems. *Waste Manag.* 15 [2], 137-148. [https://doi.org/10.1016/0956-053X\(95\)00013-P](https://doi.org/10.1016/0956-053X(95)00013-P).
  35. Tashiro, C.; Oba, J. (1979) The effects of Cr<sub>2</sub>O<sub>3</sub>, Cu (OH)<sub>2</sub>, ZnO and PbO on the compressive strength and the hydrates of the hardened C,A paste. *Cem. Concr. Res.* 9 [2], 253-258. [https://doi.org/10.1016/0008-8846\(79\)90032-2](https://doi.org/10.1016/0008-8846(79)90032-2).
  36. Poon, C.S.; Clark, A.I.; Peters, C.J.; Perry, R. (1985) Mechanisms of metal fixation and leaching by cement based fixation processes. *Sci. Total Environ.* 3 [2], 127-142. [https://doi.org/10.1016/0048-9697\(85\)90161-5](https://doi.org/10.1016/0048-9697(85)90161-5).